Forced convection of non-Newtonian fluids in porous concentric annuli

M.K. Alkam, M.A. Al-Nimr and Z. Mousa

Mechanical Engineering Department, Jordan University of Science and Technology, Irbid, Jordan

Received July 1996
Revised April 1997
Accepted March 1998

Nomenclature

C = Forchheimer constant or porous inertia coefficient, $C = 0.143\varepsilon^{-3/2}$

C_P = specific heat of the fluid (J/kg.K)

Da = Darcy number, $\dfrac{(K^*/\varepsilon)^{2/(1+n)}}{d_H^2}$

d_H = hydraulic diameter of annulus, $2(r_2 - r_1)$, (m)

K = intrinsic permeability (m^2) of porous medium

K^* = modified permeability (m^{n+1}) of porous medium for flow of power law fluids

n = power law index of inelastic Ostwald-de Waele fluid

N = annulus radius ratio, (r_1/r_2)

Nuz = local Nusselt number, $\dfrac{d_n \left.\dfrac{\partial T}{\partial r}\right|_{wall}}{T_W - T_M} = \dfrac{1}{1-\theta_m}\left.\dfrac{\partial \theta}{\partial R}\right|_{wall}$

p = fluid pressure at any cross-section, Pa

P = dimensionless pressure at any section, $\dfrac{p - p}{\left(\rho/\varepsilon^2\right)u_0^2}$

Pe^* = modified Peclet number, $\dfrac{u_o}{\alpha}\dfrac{\left(K/\varepsilon\right)^{\frac{n}{2}}}{d_H^{n-1}}$

Pr* = modified Prandtl number, $\dfrac{Pe^*}{\mathrm{Re}_\kappa}$

q_t = total heat absorbed by fluid from entrance cross-section until a point under consideration, $2\pi\rho C_P \int_{r_1}^{r_2} r u_0 (T - T_0)\,dr$

Q_t = dimensionless heat absorbed by fluid, $\dfrac{q_t}{\pi\rho C_p u_o d_H^2 (T - T_o)} = 2\int_{\frac{N}{2(1-N)}}^{\frac{1}{2(1-N)}} RU\theta\,dr$

r = radial coordinate (m)

r_1 = inner radius of the annulus

r_2 = outer radius of the annulus

R = dimensionless radial coordinate, (r/d_H)

R_1 = dimensionless inner radius

R_2 = dimensionless outer radius

Re_K = Reynolds number for power law fluid based on length scale, $(K/\varepsilon)^{1/2}.\dfrac{\rho\left(K/\varepsilon\right)^{n/2}\left(u_0/\varepsilon\right)^{2-n}}{\mu^*}$

Re^* = microscale Reynolds number based on permeability, $\dfrac{\rho C K^* u_0^{2-n}}{\mu^*\sqrt{K}}$

t = time (s)

T = temperature (K)

T_m = mixing cup temperature over any cross-section, $\dfrac{\int_{r_1}^{r_2} ruT\,dr}{\int_{r_1}^{r_2} ru\,dr}$

T_o = fluid temperature at annulus entrance (K)

T_w = heated wall temperature (K)

u = axial velocity component (m/s)

u_o = fluid axial velocity at annulus entrance (m/s)

U = dimensionless axial velocity, (u/u_o)

v = radial velocity (m/s)

V = dimensionless radial velocity, $\dfrac{d_H^2\,\mathrm{Rc}_\kappa \nu}{(K/\varepsilon)^{n/2}u_o}$

International Journal of Numerical Methods for Heat & Fluid Flow
Vol. 8 No. 6, 1998, pp. 703–716.

z = axial coordinate (m)

Z = dimensionless axial coordinate, $\frac{z(K/\varepsilon)^{n/2}}{d_n^{n+1}\,\mathrm{Re}_\kappa}$

Greek symbols

α = effective thermal diffusivity of porous medium (m^2/s)

ε = porosity of entire solid medium

θ = dimensionless temperature distribution, $\frac{T-T_o}{T_w-T_o}$

θ_m = dimensionless mixing cup temperature,

$$\frac{T-T_o}{T_w-T_o}=\frac{\int_{\frac{N}{2(1-N)}}^{\frac{1}{2(1-N)}} RU\theta dR}{\int_{\frac{N}{2(1-N)}}^{\frac{1}{2(1-N)}} RU dR}$$

μ^* = consistency index ($Pa.s^n$) of a power law fluid

ν = kinematics viscosity

ρ = fluid density (kg/m^3)

σ = effective heat capacity of the fluid-saturated porous medium $\frac{[\varepsilon\rho C_p+(1-\varepsilon)\rho_s C_{ps}]}{\rho C_p}$

τ = dimensionless time, $\frac{u_o(K/\varepsilon)^{n/2}t}{\sigma d_H^{n+1}\,\mathrm{Re}_K}$

Subscripts

s = solid

t = thermal

° = entrance cross-section

Introduction

There has been a sudden surge of interest in heat transfer in non-Newtonian fluids-saturated porous media. This is because in many engineering applications, a number of fluids exhibiting non-Newtonian behavior come in contact with porous media, particularly in enhanced oil recovery and filtration processes. Further examples of convection of non-Newtonian fluids through porous media may be found in:

(1) biomechanics where fluids flow through lungs and arteries. The blood flow is bounded by two layers held together by regularly spaced tissues that are often idealized as porous media;

(2) chemical engineering, especially in the case of packed bed reactors;

(3) ceramic engineering applications such as drying or burnout of binder systems from green compacts during colloidal processing of ceramics;

(4) the production of heavy crude oil by means of thermal methods, such as steam injection into an oil reservoir.

Using Darcy-Forchheimer model, the natural and forced convection of non-Newtonian fluid boundary-layer over a semi-infinite vertical flat plate embedded in a porous medium was investigated by Shenoy[1]. The same problem but with Darcy flow model was investigated by Chen and Chen[2] for a horizontal flat plate and for a vertical flat plate[3]. Nakayama and Shenoy[4], Nakayama and Pop[5], and Nakayama and Koyama[6] presented different similarity solutions for the problem of forced and natural convection past nonisothermal smooth surfaces of arbitrary shape embedded in non-Newtonian fluid-saturated porous medium. The mixed convection non-Newtonian fluid

flow problem past an isothermal vertical plate embedded in a porous medium was investigated by Wang *et al.*[7].

Using Brinkman-Forchheimer model, the problem of non-Newtonian forced convection fluid flow in two-parallel plates porous channels was investigated by Nakayama and Shenoy[8]. The free convection flow from a point heat source embedded in a porous medium saturated with a non-Newtonian fluid is analyzed by Nakayama[9]. The same problem but with a horizontal line heat source is solved by Nakayama[10]. Haq and Mulligan[11] and Pascal[12] have considered the transient free convection flow of a non-Newtonian fluid over a vertical plate embedded in a porous medium by using the Darcy flow model. The natural convection in a porous layer saturated with a non-Newtonian fluid and heated from below was investigated by Rudraiah *et al.*[13]. A simplified couette flow of a non-Newtonian fluid in eccentric annuli has been studied by Yang and Chukwu[14]. An excellent review was introduced by Shenoy[15] in which the reader can notice the different categories of flow and convection heat transfer models, and the achievements in each category. The transient forced convection problem of non-Newtonian fluid flow in porous annulus has not been considered yet. This problem will be the subject of the present investigation (Figure 1).

Analysis

Consider the transient fluid flow of a non-Newtonian fluid in porous annulus. The fluid and solid matrix are in local thermal equilibrium and the hydrodynamic behavior of the flow is steady. The transient behavior resulted from sudden changes in the thermal conditions of one (or more) of the channel boundaries.

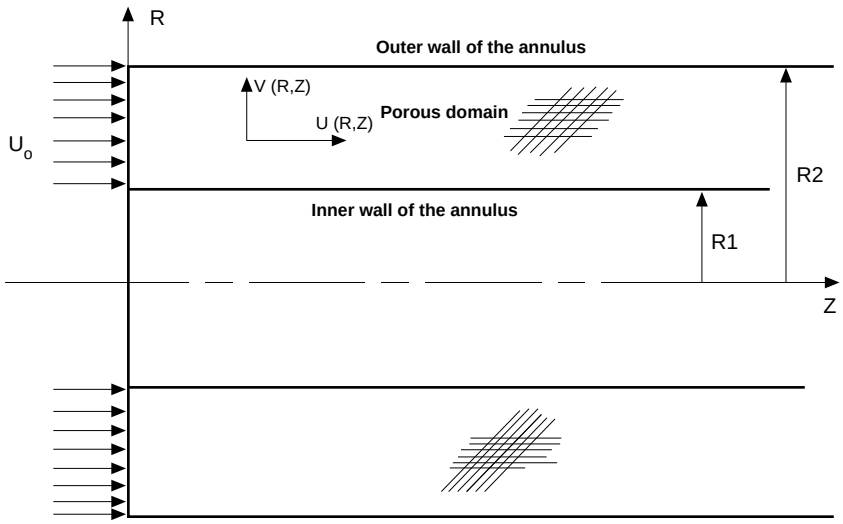

Figure 1.
Schematic diagram for the problem under consideration in dimensionless cylindrical coordinates

Using the dimensionless parameters defined in the nomenclature, the governing equations are reduced to

$$\frac{\partial U}{\partial Z}+\frac{1}{R}\frac{\partial (RV)}{\partial R}=0 \tag{1}$$

$$U\frac{\partial U}{\partial Z}+V\frac{\partial U}{\partial R}=\frac{-dP}{dZ}+\frac{1}{R}\frac{\partial}{\partial R}\left(R\left|\frac{\partial U}{\partial R}\right|^{n-1}\frac{\partial U}{\partial R}\right)-\frac{1}{Da^{\frac{n+1}{2}}}U^{n}-\frac{\mathrm{Re}^{*}}{Da^{\frac{n+1}{2}}}U^{2} \tag{2}$$

$$\frac{\partial \theta}{\partial \tau_{1}}+U\frac{\partial \theta}{\partial Z}+V\frac{\partial \theta}{\partial R}=\frac{1}{\mathrm{Pr}^{*}}\frac{1}{R}\frac{\partial}{\partial R}\left(R\frac{\partial \theta}{\partial R}\right) \tag{3}$$

Where the Darcy number, the microscale Reynolds number based on permeability and the modified Prandtl number are defined as

$$Da=\frac{\left(K^{*}/\varepsilon^{*}\right)^{2/(1+n)}}{d_{H}^{2}}$$

$$\mathrm{Re}^{*}=\frac{C\rho K^{*}u_{o}^{2-n}}{\mu^{*}\sqrt{K}}$$

$$\mathrm{Pr}^{*}=\frac{Pe^{*}}{\mathrm{Re}_{K}}$$

where

$$Pe^{*}=\frac{u_{o}}{\alpha}\frac{(K/\varepsilon)^{n/2}}{d_{H}^{n-1}}=\text{modified Peclet number}$$

$$\mathrm{Re}_{K}=\frac{\rho(K/\varepsilon)^{n/2}(u_{o}/\varepsilon)^{2-n}}{\mu^{*}}=\text{Reynolds number based on length scale, } (K/\varepsilon)^{1/2}$$

It is noteworthy that the radial momentum equation has been eliminated due to the boundary-layer simplifications. However, it is possible under the linearized numerical scheme of Bodoia and Osterle[16] to compensate for the lack of such an equation by using the following dimensionless integral continuity equation:

$$\int_{\frac{N}{2(1-N)}}^{\frac{1}{2(1-N)}}RU\,dR=\frac{(1+N)}{8(1-N)} \tag{4}$$

Equations (1-3) are subjected to the following initial conditions at $\tau = 0$:

$$\text{For } Z\geq 0 \quad \textit{and} \quad \frac{N}{2(1-N)}<R<\frac{1}{2(1-N)}$$

$$\theta=0$$

The hydrodynamic boundary conditions are given as

$$\text{At } Z = 0 \quad \text{and} \quad \frac{N}{2(1-N)} < R < \frac{1}{2(1-N)}$$

$$U = 1 \quad , V = 0$$

$$\text{For } Z > 0 \quad \text{and} \quad R = \frac{N}{2(1-N)} \quad \text{or} \quad R = \frac{1}{2(1-N)}$$

$$U = 0 \quad , V = 0$$

Two types of thermal boundary conditions are considered. These cases are as follows:

Case I

In this case, a step temperature change occurs at inner wall (isothermal wall) while the outer wall is kept adiabatic. This corresponds to:

$$\text{At } Z = 0 \text{ and } \frac{N}{2(1-N)} < R < \frac{1}{2(1-N)} : \theta = 0$$

$$\text{For } Z > 0 \text{ and } R = \frac{N}{2(1-N)} : \quad \theta = 1$$

$$\text{For } Z > 0 \text{ and } R = \frac{1}{2(1-N)} : \quad \frac{\partial \theta}{\partial R} = 0$$

Case O

In this case, a step temperature change occurs at the outer wall (isothermal wall) while the inner wall is kept adiabatic. The corresponding boundary conditions are:

$$\text{At } Z = 0 \text{ and } \frac{N}{2(1-N)} < R < \frac{1}{2(1-N)} : \theta = 0$$

$$\text{For } Z > 0 \text{ and } R = \frac{N}{2(1-N)} : \frac{\partial \theta}{\partial R} = 0$$

$$\text{For } Z > 0 \text{ and } R = \frac{1}{2(1-N)} : \theta = 1$$

Numerical method of solution

In the current investigation, the flow is assumed to be axisymmetric, and hence, half of the R-Z domain is considered for computational purposes. The spatial grid is generated over the domain of interest while the nondimensional time, τ, is simulated as a third coordinate normal to the R-Z plane. The governing equations are discretized by an implicit finite difference scheme. In this scheme,

the radial derivatives in the governing equations are discretized by central difference formulas, and a first order backward scheme is used for both the axial and time derivatives. The consistency and stability of the discretized governing equations have been checked, and it is found that the derived forms are consistent and stable as long as the downstream axial velocity U is non-negative, i.e. there is no flow reversal within the domain of the solution.

The method discussed by Bodoia and Osterle[16] is used to solve the finite difference equations that simulate the flow hydrodynamics at steady state conditions. Having obtained the values of U, V, over the flow field, the discretized energy equations are solved by marching in time. The solution procedure in time is carried out until steady-state conditions are practically achieved. The steady state conditions are declared when the summation of the residue over the cross section reaches a value less than 1×10^{-4}. The residue is defined as the absolute difference in temperature between a grid point and the previous one in time direction.

In order to obtain a solution independent of the grid size, several runs were performed to obtain the optimum step sizes in R, Z, and τ directions. The optimization procedure of the grid size includes computing the radial temperature distribution at an arbitrary location, employing a given number of grid points in both the radial and axial directions. After that the number of grid points is increased gradually, and each time, a computer run is performed to compute the temperature profile. A residue is defined as the absolute difference in temperature between the computed temperature distribution and the one obtained in the previous run. The procedure is continued until the residue approaches a value less than 1×10^{-4}. At this point the special grid size is fixed. A similar procedure is followed to choose the optimum time step. The optimum choice was $\Delta R = 0.02$, $\Delta Z = 0.1$ and $\Delta\tau = 0.01$.

Results and discussion

The computations are carried out for the following values of the flow and geometry parameters:

$N = 0.5$, $Da = 0.001$ and 0.01;

$Re^* = 0.0$, 10.0 and 100.0;

$Pr^* = 0.1$, 1.0 and 10.0.

In order to validate the present code, a special computer run was made with different Da numbers, and $n = 1.0$ for case I. These operating conditions represent the Newtonian fluid flow in the developing region of a porous annulus. In the limit of $Da >> 1.0$ (i.e. $Da = 100$), the operating conditions represent the Newtonian fluid flow in the developing region of a clear (nonporous) annulus. This special case is considered by El-Shaarawi and Alkam[17]. The radial temperature profiles obtained from the present code are compared in Figure 2 with those obtained by El-Shaarawi and Alkam[17]. The

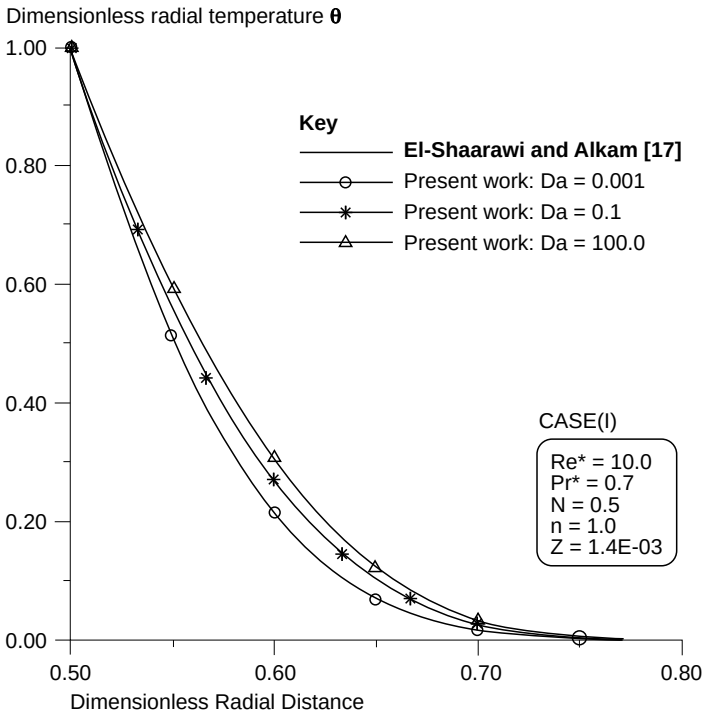

Figure 2.
Comparison between the present work and El-Shaarawi and Alkam[17], for radial temperature profiles

figure shows an acceptable match between the result of the present work and the results of El-Shaarawi and Alkam[17].

The effect of Da, Re^*, and Pr^* numbers on the axial variation of Nu_z are shown in Figures 3 and 4 for case I heating condition. Owing to the thickening of both hydrodynamics and thermal boundary layers in the downstream direction, the thermal resistance of the boundary layer increases and as a result, Nu_z number decreases. Now, increasing Re^* reduces the hydrodynamic boundary layer thickness and improves Nusselt number. Also, it is clear from Figures 3 and 4 that fluids of higher Pr^* yield higher Nusselt numbers Nu_z. In fact all the correlations in forced convection heat transfer assume that $Nu_z \propto Pr^*$. On the other hand the effect of Re^* on Nu_z becomes greater as the value of Pr* increases. A comparison between Figures 3 and 4 shows that as the Darcy number decreases, the Nusselt number increases.

Figure 5 describes the effect of the power law index n on the Nusselt number value for case I. Increasing n leads to a reduction in the Nusselt number. As n increases, the shear stress increases, and hence, the flow experiences more retardation. The increase in the shear stress enlarges the boundary layer region which acts as an insulation to the heat flux. The result is a decrease in Nu_z. An important result from the same figure is the fact that n has a small effect on Nu_z in the fully developed region compared to the developing region.

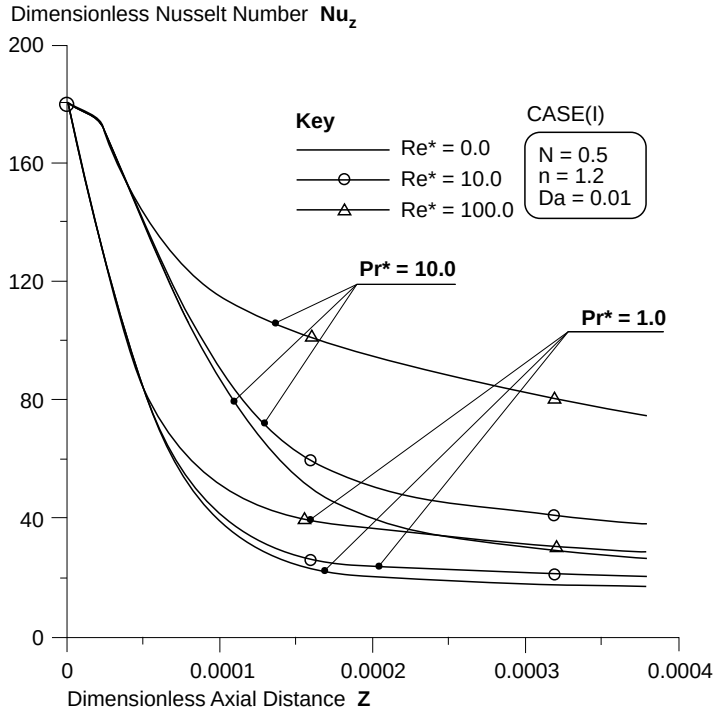

Figure 3.
Dimensionless Nusselt number vs. axial distance at steady state time for Da = 0.01

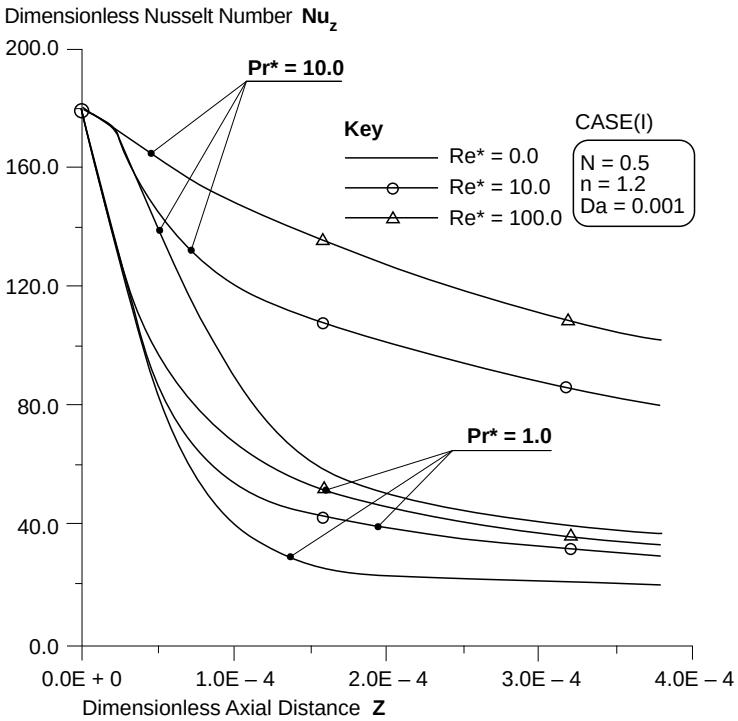

Figure 4.
Dimensionless Nusselt number vs. axial distance at steady state time for Da = 0.001

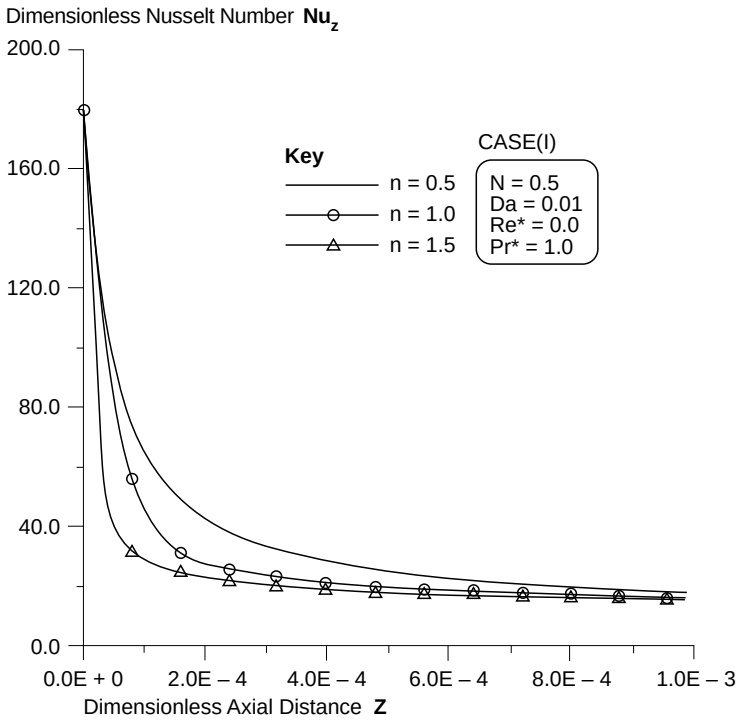

Figure 5.
Dimensionless Nusselt number vs. axial distance at steady state time for different values of "n"

The effects of both Re^* and Da numbers on the dimensionless heat absorbed and for different heating conditions are shown in Figures 6-9. Higher Re^* leads to higher total heat absorbed due to the improvement in Nu_z. Also, case O predicts much higher total heat absorbed than case I due to its larger surface area. As Darcy number decreases, the heat absorbed by the fluid increases. This is due to the improvement in Nu_z.

The effects of Re^* and Pr^* on the thermal entrance length under steady state conditions are shown in Figure 10. Increasing Re^* increases the entrance length. This is due to the reduction in the hydrodynamic and thermal boundary layers which occurs as a result of increasing Re^*. Owing to the reduction in their thickness, the thermal boundary layers need a longer distance to meet. Also, it is clear that fluids of higher Pr^* have higher entrance thermal lengths due to the fact that fluids of higher Pr^* have much thinner thermal boundary layers than those of lower Pr^*. As a result, higher Pr^* fluids need longer axial distances to attain thermally fully developed states. Another conclusion reached from the same figure is that, the entrance length of case I is longer than that for case O for the same Pr^* because the boundary layer is thinner in case I. The effect of Da on the thermal entrance length is shown in Figure 11. Increasing Da reduces the thermal entrance length.

The effect of the power law index "n" on the thermal entrance length is shown in Figure 12 for the two cases I and O. As is clear from this figure that

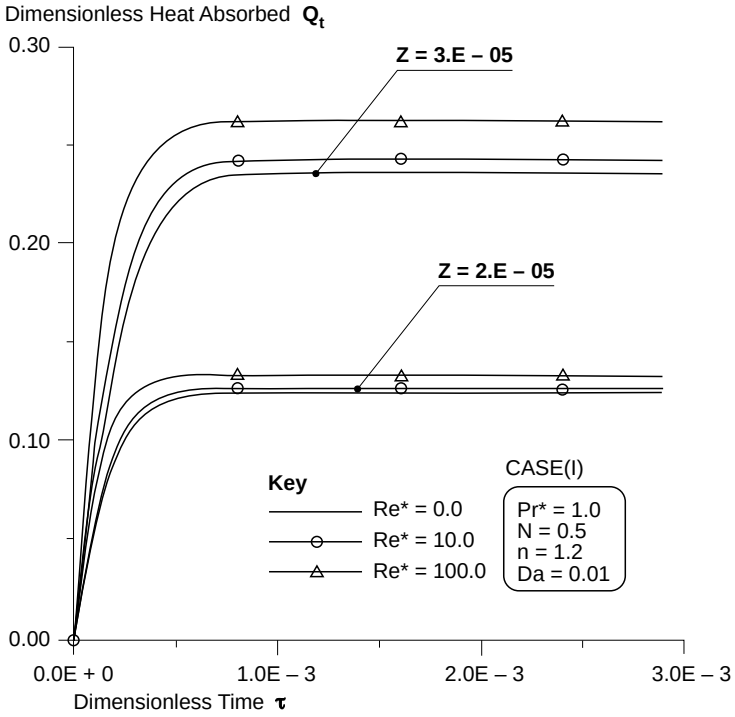

Figure 6.
Dimensionless heat absorbed vs. dimensionless time for case (I) with Da = 0.01

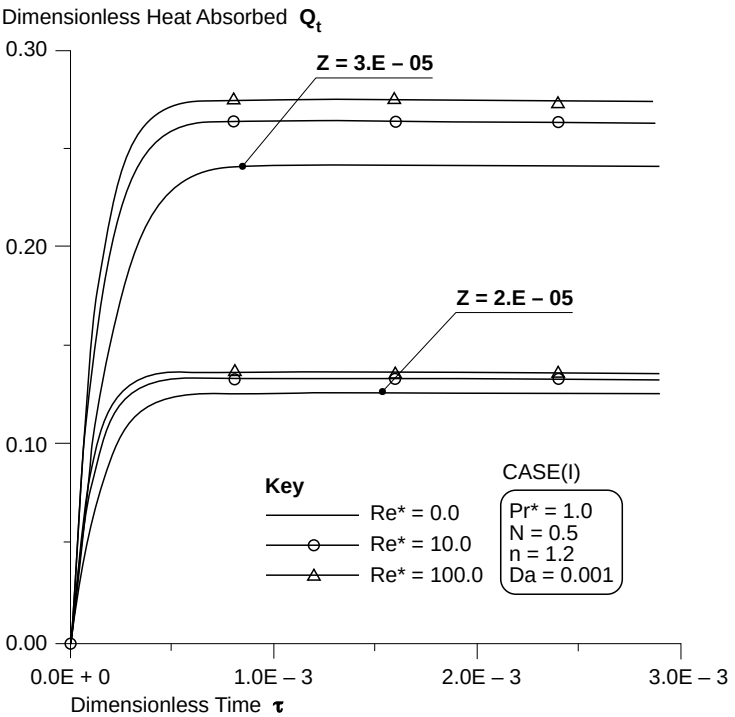

Figure 7.
Dimensionless heat absorbed vs. dimensionless time for case (I) with Da = 0.001

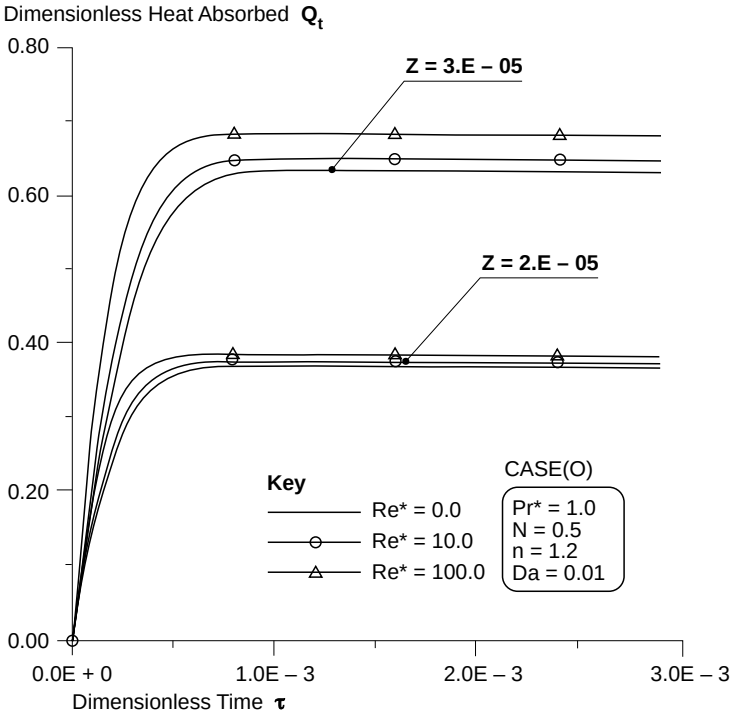

Figure 8.
Dimensionless heat absorbed vs. dimensionless time for case (O) with Da = 0.01

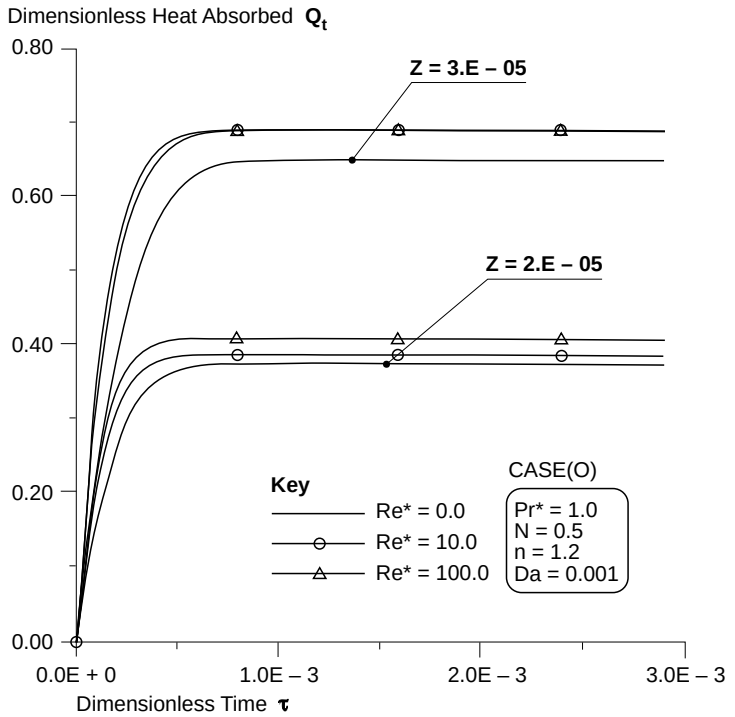

Figure 9.
Dimensionless heat absorbed vs. dimensionless time for case (O) with Da = 0.001

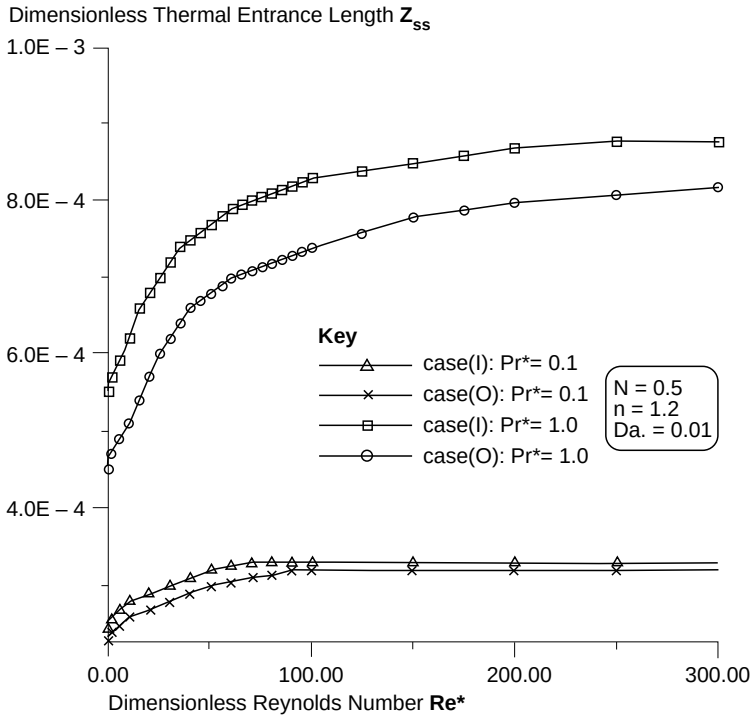

Figure 10.
Dimensionless thermal entrance length vs. dimensionless Re^*

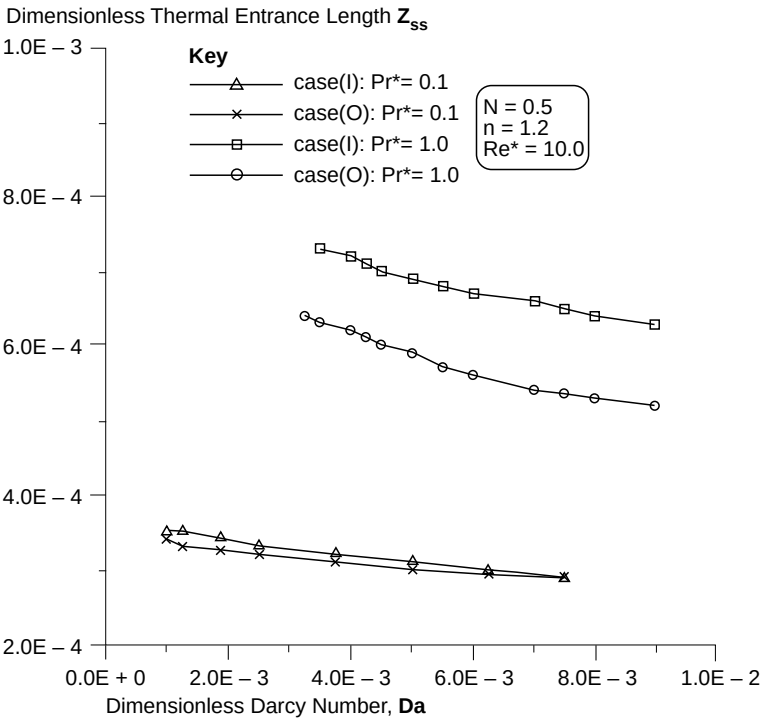

Figure 11.
Dimensionless thermal entrance length vs. dimensionless Da

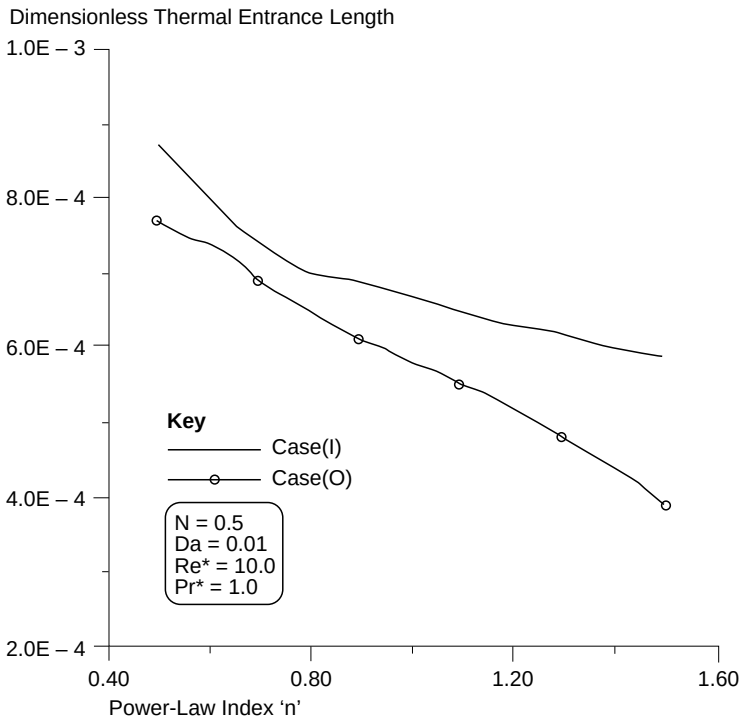

Figure 12.
The effect of the power-law index on the thermal entrance length for cases (I) and (O)

increasing n reduces the thermal entrance length. This is due to the fact that fluids of larger n have thicker thermal and hydrodynamic boundary layers, as concluded from Figure 5, and as a result, they have a shorter thermal entrance length.

Conclusions

A numerical investigation for the transient forced convection problem of non-Newtonian fluid flow in the entrance region of porous concentric annuli is carried out. The effect of four important parameters, which are Re^*, Pr^*, Da, and n, on the thermal behavior of the channel is investigated. The thermal behavior of the channel is described by two important aspects which are Nusselt number and the thermal entrance length. It is found that increasing Re^* or Pr^* increases Nu_z number and the thermal entrance length. On the other hand increasing Da or n decreases Nu_z number and the thermal entrance length. The effects of the previous four parameters are investigated for two fundamental types of thermal boundary conditions. In these fundamental cases it is found that imposing the heating condition on the outer cylinder (case O) of the annuli yields much higher total heat absorbed and much shorter thermal entrance length than that predicted when the heat flux is imposed on the inner cylinder (case I).

References

1. Shenoy, A.V., "Darcy-Forchheimer natural, forced and mixed convection heat transfer in non-Newtonian power-law fluid-saturated porous media", *Trans. Porous Media*, Vol. 11, 1992, pp. 219-41.
2. Chen, T. and Chen, C.K., "Natural convection of non-Newtonian fluids about a horizontal surface in a porous medium", *Trans. ASME J. Resources Tech.*, Vol. 109, 1987, pp. 119-23.
3. Chen, T. and Chen, C.K., "Free convection of non-Newtonian fluids along a vertical plate embedded in a porous medium", *Trans. ASME, J. Heat Transfer*, Vol. 110, 1988, pp. 257-60.
4. Nakayama, A. and Shenoy, A.V., "A unified similarity transformation for Darcy and non-Darcy forced, free and mixed convection heat transfer in non-Newtonian inelastic fluid-saturated porous media", *Chem. Eng. J.*, Vol. 50, 1992, pp. 33-45.
5. Nakayama, A. and Pop, I., "A unified similarity transformation for free, forced and mixed convection in Darcy and non-Darcy porous media", *Int. J. Heat Mass Transfer*, Vol. 34, 1991, pp. 357-67.
6. Nakayama, A. and Koyama, H., "A general similarity transformation for combined free and forced convection flows within a fluid-saturated porous medium", *Trans. ASME, J. Heat Transfer*, Vol. 109, 1987, pp. 1041-5.
7. Wang, C., Tu, C. and Zhang, X., "Mixed convection of non-Newtonian fluids form a vertical plate embedded in a porous medium", *Acta Mech. Sinice*, Vol. 6, 1990, pp. 214-20.
8. Nakayama, A. and Shenoy, A.V., "Non-Darcy forced convection heat transfer in a channel embedded in a non-Newtonian inelastic fluid-saturated porous medium", *Can. J. Chem. Eng.*, Vol. 71, 1993, pp. 168-73.
9. Nakayama, A., "A similarity solution for free convection from a point heat source embedded in a non-Newtonian fluid-saturated porous medium, *Trans. ASME, J. Heat Transfer*, Vol. 115, 1993, pp. 510-13.
10. Nakayama, A., "Free convection from a horizontal line heat source in a power-law fluid-saturated porous medium", *Int. J. Heat Fluid Flow*, Vol. 14, 1993.
11. Haq and Mulligan, J.C., "Transient free convection form a vertical plate to a non-Newtonian fluid in a porous medium", *J. Non-Newtonian Fluid Mechanics*, Vol. 36, 1990, pp. 395-410.
12. Pascal, H., "Rheological effects of non-Newtonian fluids on natural convection in a porous medium", *Can. J. Phys.*, Vol. 68, 1990, pp. 1456-63.
13. Rudraiah, N., Kjaloni, P.N. and Radhadevi, P.V., "Oscillatory convection in a viscoelastic fluid through a porous layer heated from below", *Rheol. Acta*, Vol. 28, 1989, pp. 48-53.
14. Yang, L. and Chukwu, G.A., "A simplified couette flow solution of non-Newtonian power-law fluids in eccentric annuli", *Can. J. Chem. Eng.*, Vol. 73, 1995, pp. 241-7.
15. Shenoy, A.V., "Non-Newtonian fluid heat transfer in porous media", *Advances in Heat Transfer*, Vol. 24, 1994, pp. 101-90.
16. Bodoia, J.R. and Osterle, J.F., "Finite-difference analysis of plane Poiseuille and Couette flow developments", *Apl. Sci. Res. Alo.*, 1961, pp. 265-76.
17. El-Shaarawi and Alkam, M.K., "Transient forced convection in the entrance region of concentric annuli", *Int. J. Heat Mass Transfer*, Vol. 35, 1992, pp. 3335-44.